Chapter 5
Seasonality

5.1 Environmental Drivers

Host behavior and environmental factors influence disease dynamics in a variety of ways through affecting the parasite/pathogen—the survival of infective stages outside the host, speed of development of free-living stages, etc.; and the host population—changing birth-rates, carrying capacity, social organization, etc. Sometimes such influences have relatively subtle consequences (e.g., slight changes in R_0) as is likely the effect of absolute humidity on influenza transmission (Lowen et al. 2007). Other times the consequences are substantial by changing the dynamics qualitatively such as inducing multiannual or chaotic epidemics (Dalziel et al. 2016) or initiating ecological cascades (Jones et al. 1998; Glass et al. 2000). It is useful to distinguish between trends, predictable variability (such as seasonality), and non-predictable variability due to "environmental" and "demographic" stochasticity (see Chap. 7).

Some level of seasonality in transmission is very common in infectious disease dynamics and is usually reflected in seasonal cycles in incidence (Altizer et al. 2006); Seasonality in *incidence* is the norm even for persistent infections for which prevalence may remain relatively stable. Influenza is the poster-child for seasonality in infection risk in the public eye (e.g., Bjørnstad and Viboud 2016). Figure 5.1a shows the mean weekly influenza-related deaths in Pennsylvania between 1972 and

This chapter uses the following R-packages: `deSolve` and `plotrix`.
A conceptual understanding of *seasonality* is useful prior to this discussion. A 5-min epidemics-MOOC can be seen on YouTube: https://www.youtube.com/watch?v=TDuuM-wm6nw.

O. N. Bjørnstad, *Epidemics*, Use R!, https://doi.org/10.1007/978-3-319-97487-3_5

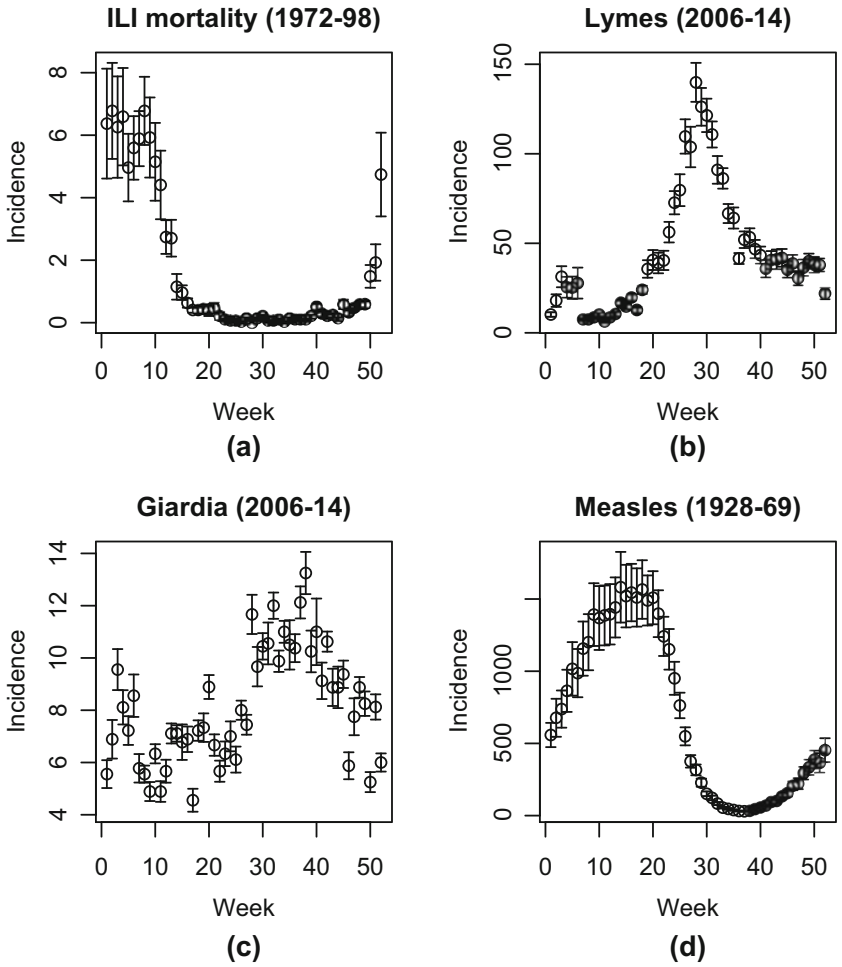

Fig. 5.1 Mean (± 1 SD) weekly incidence of (**a**) deaths due to influenza like illness, (**b**) Lyme's disease, (**c**) giardiosis, and (**d**) pre-vaccination measles in Pennsylvania

1998. The pronounced winter-peaked seasonality is not fully understood, but are thought to be linked to how climate conditions—notably absolute humidity (Shaman and Kohn 2009)—affect rates of viral degradation outside the host.

We can illustrate various types of seasonality using four diseases in Pennsylvania contained in the `paili`, `palymes`, `pagiard`, and `pameasle` data sets. We first write a simple function to extract and plot weekly average incidence (and standard errors) through the year from time series. Weekly incidence data occasionally has 53 reporting weeks (because years are 52.14 weeks, and leap years are 52.28 weeks). The function omits these extras.

```
ppp=function(wk, x){
require(plotrix)
x=x[wk<53]
wk=wk[wk<53]
ses=sapply(split(x, wk), mean, na.rm=TRUE)
sesdv=sapply(split(x, wk), sd, na.rm=
     TRUE)/sqrt(length(split(x, wk)))
plotCI(x=c(1:52), y=ses, ui=ses+sesdv,
     li=ses-sesdv, xlab="Week", ylab="Incidence")
}
```

We apply the function to influenza-like illness, Lyme's disease, giardiosis, and measles (Fig. 5.1):

```
par(mfrow = c(2, 2))  #A four panel plot
ppp(paili[, "WEEK"], paili[, "PENNSYLVANIA"])
title("ILI mortality (1972-98)")
ppp(palymes[, "WEEK"], palymes[, "PENNSYLVANIA"])
title("Lymes (2006-14)")
ppp(pagiard[, "WEEK"], pagiard[, "PENNSYLVANIA"])
title("Giardia (2006-14)")
ppp(pameasle[, "WEEK"], pameasle[, "PENNSYLVANIA"])
title("Measles (1928-69)")
```

Seasonality arises from a variety of causes depending on the mode of transmission of the pathogen: air-borne (like influenza), vector-borne, or water/food-borne. Lyme's disease, for example, is caused by tick-vectored bacteria in the genus *Borrelia*. Figure 5.1b shows the sharply seasonal incidence of human cases of Lyme's in Pennsylvania between 2006 and 2014. The seasonality is the combined effect of seasonality in tick activity levels and human use of wilderness. Most mosquito-vectored pathogens also show strong seasonality because of the temperature- and precipitation-dependence of the vector life cycle. The seasonality of cholera infections, caused by the *Vibrio cholerae* bacterium, is among the most studied water-borne pathogens. The seasonality in southeast Asia is caused by rainfall variation associated with the monsoon season (Codeço 2001; Ruiz-Moreno et al. 2007) (Fig. 1.3b). However, other water-borne diseases like giardiasis also show marked seasonality (Fig. 5.1c). Host behavior can further cause seasonality in contact rates. Childhood disease dynamics, for example, are often shaped by "term-time" forcing: increased transmission when schools are open (e.g., Fine and Clarkson 1982; Kucharski et al. 2015). Weekly average pre-vaccination incidence of measles in Pennsylvania, for instance, collapses as school closes for the summer only to resume robust circulation after the vacation end (Fig. 5.1d). Additionally, seasonal urban-rural migration in Niger has been shown to generate strong seasonality in measles transmission (Ferrari et al. 2008). Seasonally varying birth rates can induce seasonality in susceptible recruitment in wildlife (Peel et al. 2014) and humans (Martinez-Bakker et al. 2014).

5.2 The Seasonally Forced SEIR Model

To study the effect of seasonality in transmission we will modify the SEIR model (Eqs. (3.3)–(3.5)). We first define the gradient functions for the "undriven" system:

```
seirmod = function(t, y, parms) {
    S = y[1]
    E = y[2]
    I = y[3]
    R = y[4]

    mu = parms["mu"]
    N = parms["N"]
    beta = parms["beta"]
    sigma = parms["sigma"]
    gamma = parms["gamma"]

    dS = mu * (N - S) - beta * S * I/N
    dE = beta * S * I/N - (mu + sigma) * E
    dI = sigma * E - (mu + gamma) * I
    dR = gamma * I - mu * R
    res = c(dS, dE, dI, dR)
    list(res)
}
```

We simulate 10 years of dynamics using the basic recipe introduced in Sect. 2.2. The seasonally forced SEIR model has been very successfully applied to understand the dynamics of measles (and other immunizing childhood infections). To simulate measles-like dynamics we assume a latent period of 8 days and an infectious period of 5 days. We assume the initial host population to be 0.1% infectious, 6% susceptibles, and the rest immune; The R_0 of measles is typically quoted in the 13–20 range, which means that the equilibrium fraction of susceptibles is somewhere around 5%. For simplicity we assume a host life span of 50 years and set $N = 1$ to model the fraction in each compartment.

```
require(deSolve)
times  = seq(0, 10, by=1/120)
paras  = c(mu = 1/50, N = 1, beta =  1000,
     sigma = 365/8, gamma = 365/5)
start = c(S=0.06, E=0, I=0.001, R = 0.939)
```

As discussed in Sect. 3.7, the R_0 for this system—assuming disease induced mortality is negligible—is $\frac{\sigma}{\sigma+\mu}\frac{\beta}{\gamma+\mu}$. We can verify that our choice of β places R_0 in the "measles-like" range. We use `expression` to define the equation for R_0. As in

Sect. 4.8, we use `with(as.list(...))` to evaluate the expression using the definitions in the `paras`-vector.

```
R0 = expression(sigma/(sigma + mu) * beta/(gamma + mu))
with(as.list(paras), eval(R0))

  ## [1] 13.68888
```

We integrate the ODEs and plot the time series and the phase plane (Fig. 5.2). As is the case with the SIR model, the unforced SEIR model predicts dampened oscillations toward the endemic equilibrium.

```
out = as.data.frame(ode(start, times, seirmod, paras))
par(mfrow = c(1,2))  #Two plots side by side
plot(times, out$I, ylab = "Prevalence",
     xlab = "Time", type = "l")
plot(out$S, out$I, ylab = "Prevalence",
     xlab = "Susceptible", type = "l")
```

5.3 Seasonality in β

The predicted dampened oscillations toward an equilibrium is at odds with the recurrent outbreaks seen in many immunizing infections (e.g., Fig. 1.4). Sustained oscillations require either additional predictable seasonal drivers—the topic of this chapter—or stochasticity (Sect. 7.1). An important driver in human childhood infections is seasonality in contact rates because of aggregation of children during the school term (Fine and Clarkson 1982; Kucharski et al. 2015). For simplicity we can analyze the consequences of seasonality by assuming sinusoidal forcing on the transmission rate[1] according to $\beta(t) = \beta_0(1+\beta_1 cos(2\pi t))$. The mean transmission rate is β_0 but the realized transmission varies cyclically with a period of one time unit, and the magnitude of the seasonal variation is controlled by the parameter β_1. The modified gradient function is:

```
seirmod2=function(t, y, parms){
  S=y[1]
  E=y[2]
  I=y[3]
  R=y[4]
  with(as.list(parms),{
```

[1] It is possible to analyze more realistic patterns of seasonality, such as a more explicit "term-time" forcing; see Keeling et al. (2001) and Chap. 7. The qualitative (but not detailed) results appear to be robust to the exact shape of the forcing function.

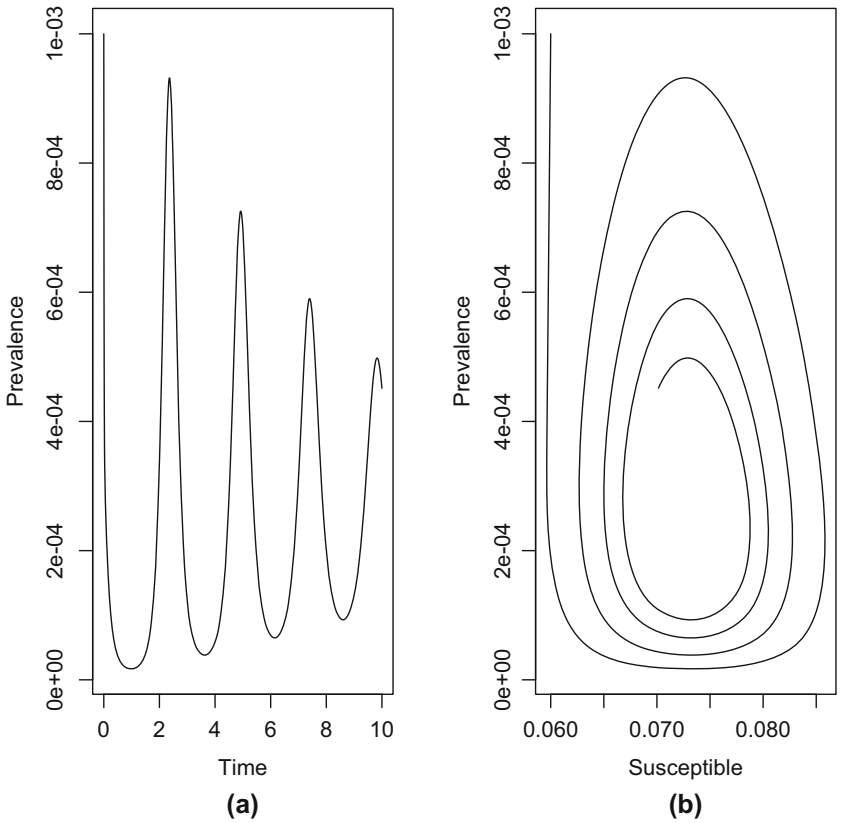

Fig. 5.2 Predicted prevalence from the SEIR model (**a**) in time, and (**b**) in the phase plane with $\mu = 1/50$, $N = 1$ (to model fractions), $\beta = 1000$, $\sigma = 365/8$, and $\gamma = 365/5$. Ten years are not long enough for the simulation to settle on the endemic equilibrium

```
      dS = mu * (N  - S)  - beta0 * (1+beta1 *
         cos(2 * pi * t)) * S * I / N
      dE = beta0 * (1 + beta1 * cos(2*pi * t)) *
         S * I / N - (mu + sigma) * E
      dI = sigma * E - (mu + gamma) * I
      dR = gamma * I - mu * R
      res=c(dS, dE, dI, dR)
      list(res)
    })
}
```

With no seasonality the model predicts dampened oscillation, with moderate seasonality the prediction is low-amplitude annual outbreaks. However, as seasonality increases (to $\beta_1 = 0.2$, say) we start seeing some surprising consequences of the sea-

sonal forcing (Fig. 5.3): the appearance of harmonic resonance between the internal cyclic dynamics of the SEIR clockwork and the annual seasonal forcing function.

```
times  = seq(0, 100, by=1/120)
paras  = c(mu = 1/50, N = 1, beta0 = 1000, beta1 = 0.2,
     sigma = 365/8, gamma = 365/5)
start = c(S=0.06, E=0, I=0.001, R = 0.939)
out = as.data.frame(ode(start, times, seirmod2, paras))
par(mfrow=c(1,2)) #Side-by-side plot
plot(times, out$I, ylab="Infected", xlab="Time",
     xlim=c(90, 100), ylim=c(0,
     max(out$I[11001:12000])), type="l")
plot(out$S[11001:12000], out$I[11001:12000],
     ylab="Infected", xlab="Susceptible", type="l")
```

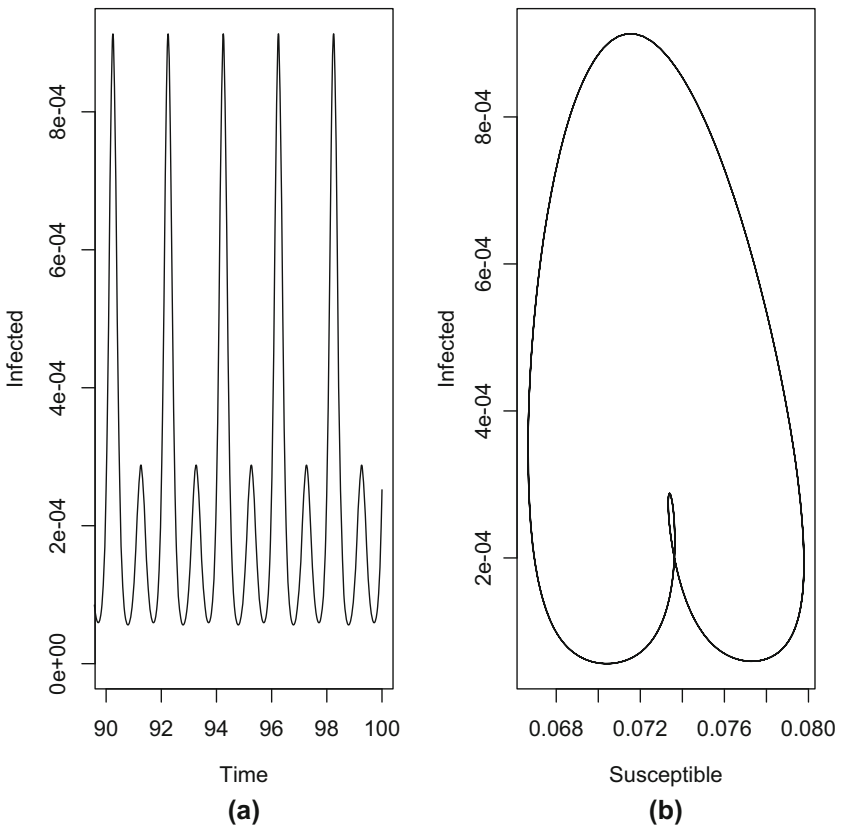

Fig. 5.3 The 10 last years of the forced SEIR model for $\beta_1 = 0.2$. (**a**) Predicted prevalence and (**b**) the S-I phase plane

The emergent pattern of recurrence in the forced SEIR is the result of an interaction between the internal periodic clockwork (the "damping period") of the SEIR flow and the externally imposed periodic forcing. The damping period is the focus of Chap. 9; however, we can use the results previewed in Sect. 2.6: When working with a continuous-time ODE model which results in cyclic behavior like the SEIR model, the dominant eigenvalues of the Jacobian matrix—when evaluated at the equilibrium—are a conjugate pair of complex numbers $(a \pm bi)$ that determines the period of the cycle according to $2\pi/b$.

The endemic equilibrium of the SEIR model is (ignoring the absorbing R compartment): $S^* = 1/R_0$, $I^* = \mu(1 - 1/R_0)R_0/\beta$ and $E^* = (\mu + \gamma)I^*/\sigma$. We first calculate the endemic equilibrium:

```
mu = paras["mu"]
N = paras["N"]
beta0 = paras["beta0"]
beta1 = paras["beta1"]
sigma = paras["sigma"]
gamma = paras["gamma"]
R0 = sigma/(sigma + mu) * beta0/(gamma + mu)

Sstar = 1/R0
Istar = mu * (1 - 1/R0) * R0/beta0
Estar = (mu + gamma) * Istar/sigma

eq = list(S = Sstar, E = Estar, I = Istar)
```

We next use Rs inbuilt D-function to carry out symbolic differentiation, and to generate and evaluate the Jacobian matrix (ignoring the absorbing R compartment):

```
dS = expression(mu * (N  - S)  - beta0 * S * I / N)
dE= expression(beta0 * S * I / N - (mu + sigma) * E)
dI = expression(sigma*E - (mu + gamma) * I)

j11 = D(dS, "S");  j12 = D(dS, "E");  j13 = D(dS, "I")
j21 = D(dE, "S");  j22 = D(dE, "E");  j23 = D(dE, "I")
j31 = D(dI, "S");  j32 = D(dI, "E"); j33 = D(dI, "I")

J=with(eq,
matrix(c(eval(j11),eval(j12),eval(j13),
   eval(j21),eval(j22), eval(j23),
   eval(j31),eval(j32), eval(j33)),
    nrow=3, byrow=TRUE))
```

We finally calculate the eigenvalues. The dominant pair of complex conjugates is at the second and third place in the vector of eigenvalues. The associated resonant period is:

```
round(eigen(J)$values, 3)

  ## [1] -118.725+0.000i   -0.107+2.667i   -0.107-2.667i

2 * pi/(Im(eigen(J)$values[2]))

  ## [1] 2.355891
```

So the recurrent biennial epidemics are sustained because the internal epidemic clock-work cycles with a period of 2.3 years, but it is forced at an annual time scale, so as a "compromise" the epidemics are locked on to the annual clock, but with alternating major and minor epidemics such as seen, for example, in pre-vaccination measles in New York 1944–1958 (Fig. 1.4b) and London 1950–1965 (Fig. 1.4c).

5.4 Bifurcation Analysis

We can make a more comprehensive summary of the consequences of seasonality on the SEIR-flow using a bifurcation analysis: a systematic search across a range of β_1 values. For annually forced models we study the dynamics by "strobing" the system once each year. To study the long-term (asymptotic) dynamics we discard the initial transient part of the simulation. In the below we hence use one data point per year for the last 42 years of simulation—which the `sel` variable flags—so that an annual cycle produces a single value (so will a fixed-point equilibrium), biannual cycles two values, etc. The resultant bifurcation plot shows when annual epidemics gives way to biannual cycles and finally chaotic dynamics as seasonality increases (Fig. 5.4). The irregular dynamics with strong seasonality comes about because there is no simple resonant compromise between the internal clock and the external forcing function. We may think of it as "resonance" giving place to "dissonance" in the dynamical system. That stronger seasonality pushes measles from regular to irregular epidemics has been predicted by the theoretical literature (e.g., Aron and Schwartz 1984) and is supported by an empirical comparison of measles in pre-vaccination UK *versus* USA by Dalziel et al. (2016) (see Sect. 10.2).

We define initial conditions and the sequence of parameter values to be considered for β_1 and then do the numerical integration for each parameter set:

```
times = seq(0, 100, by = 1/120)
start = c(S = 0.06, E = 0, I = 0.001, R = 0.939)
beta1 = seq(0,0.25, length=101)
```

```
#Matrix to store infecteds
Imat = matrix(NA, ncol = 12001, nrow = 101)
#Loop over beta1's
for(i in 1:101){
     paras  = c(mu = 1/50, N = 1, beta0 = 1000,
        beta1=beta1[i], sigma = 365/8, gamma = 365/5)
     out = as.data.frame(ode(start, times,
        seirmod2, paras))
     Imat[i,] = out$I
}
```

For the visualization we select one observation per year for the last 42 years of simulation and plot the values against the associated β_1 values (Fig. 5.4).

```
sel = seq(7001, 12000, by = 120)
plot(NA, xlim = range(beta1), ylim = c(1E-7,
     max(Imat[,sel])), log="y", xlab="beta1",
     ylab="prevalence")
for(i in 1:101){
       points(rep(beta1[i], length(sel)),
          Imat[i, sel], pch=20)
}
```

5.5 Stroboscopic Section

Rand and Wilson (1991) studied the seasonally forced SEIR model with a particular set of parameters resulting in chaotic dynamics. It is interesting to integrate the model with these parameters for a very long time (in this case for 10,000 years) to better understand/visualize the meaning of quasi-periodic chaos. Figure 5.5 shows a time series of prevalence and the dynamics in the S-I phase plane strobed at the annual time scale—the annual "stroboscopic section" of the S-I plane. The time series is erratic, but the paired S-I series trace out a very intricate pattern (Fig. 5.5b): The four-armed shape corresponds to the propensity of the chaotic pattern to adhere to a wobbly ("quasiperiodic") 4-year recurrence. We will revisit on this attractor and its role in facilitating "chaotic stochasticity" and "stochastic resonance" in disease dynamics in Chap. 10.

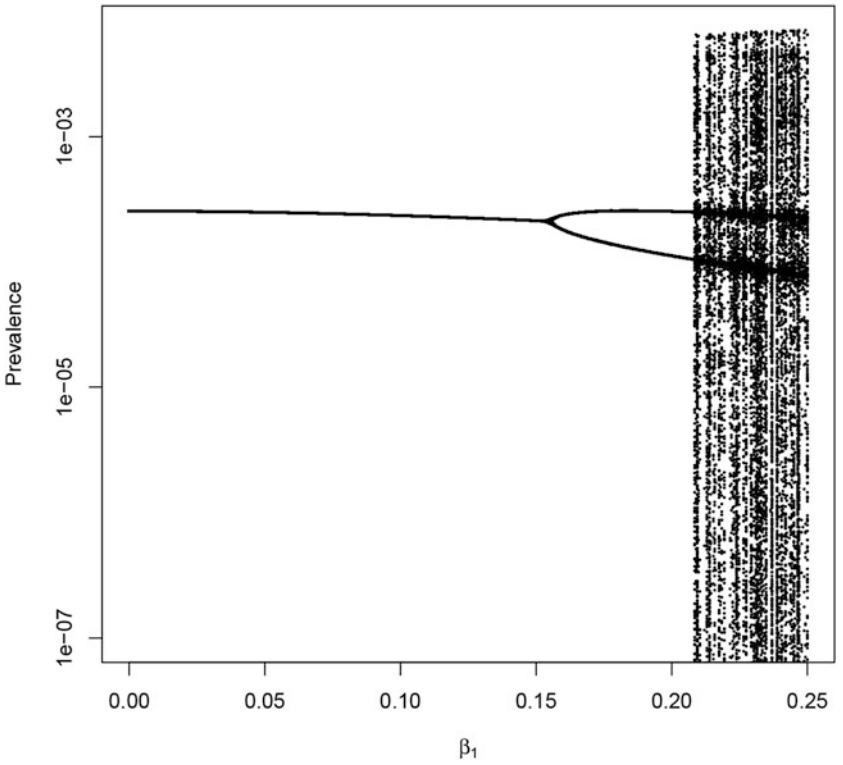

Fig. 5.4 The bifurcation plot of prevalence against seasonality for the forced SEIR model

```
times = seq(0, 100000, by = 1/120)
start = c(S = 0.06, E = 0, I = 0.001, R = 0.939)
paras  = c(mu = 1/50, N = 1, beta0 = 1800, beta1=0.28,
     sigma = 35.84, gamma = 100)
out = as.data.frame(ode(start, times,seirmod2, paras))
sel=seq(7001, 12000000, by=120)
par(mfrow=c(1,2))
plot(out$time[7001:13001], out$I[7001:13001],
     type="l", xlab="Year", ylab="Prevalence")
plot(out$S[sel], out$I[sel], type="p", xlab="S",
     ylab="I", log="y", pch=20, cex=0.25)
```

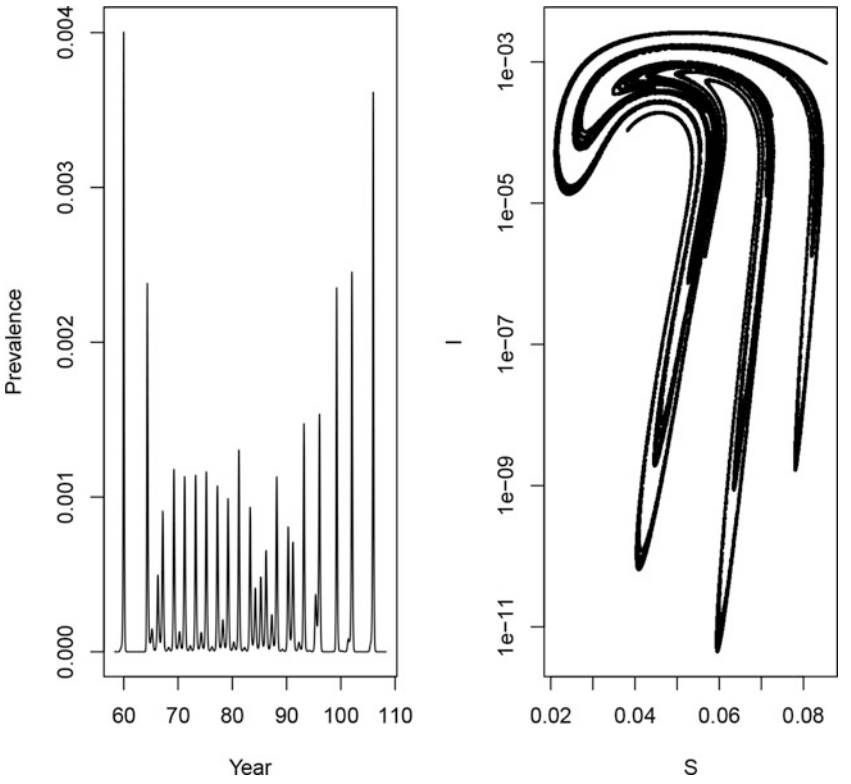

Fig. 5.5 Stroboscopic section in the S-I phase plane of the quasiperiodic chaotic prevalence of the seasonally forced SEIR model ($\mu = 0.02$, $\beta_0 = 1800$, $\beta_1 = 0.28$, $\sigma = 35.84$, $\gamma = 100$) (Rand and Wilson 1991)

5.6 Susceptible Recruitment

The patterns of recurrent epidemics are also shaped by other characteristics of the host and pathogen. Earn et al. (2000b) studied how susceptible recruitment affects dynamics of the seasonally forced SEIR model by doing a bifurcation analysis over μ (Fig. 5.6). As concluded by Earn et al. (2000b), reduced susceptible recruitment in the seasonally forced SEIR model leads to a cascade from annual to biennial to coexisting annual and complex attractors. To trace out the coexisting attractors it is necessary to use multiple starting conditions because each attractor will have its own "basin of attraction." We do this by looping forwards and backwards over μ using the final values of the previous simulation as initial conditions for the next.

```
times = seq(0, 100, by = 1/120)
start = c(S = 0.06, E = 0, I = 0.001, R = 0.939)
mu=seq(from = 0.005, to = 0.02, length = 101)
ImatF=ImatB=matrix(NA, ncol = 12001, nrow = 101)
```

```
for(i in 1:101){
     paras  = c(mu = mu[i], N = 1, beta0 = 2500,
          beta1=0.12, sigma = 365/8, gamma = 365/5)
      out = as.data.frame(ode(start, times, seirmod2,
           paras))
      ImatF[i,]=out$I
      start = c(S = out$S[12001], E = out$E[12001],
           I = out$I[12001], R = out$R[12001])
}
start = c(S = 0.06, E = 0, I = 0.001, R = 0.939)
for(i in 101:1){
     paras  = c(mu = mu[i], N = 1, beta0 = 2500,
          beta1=0.12, sigma = 365/8, gamma = 365/5)
     out = as.data.frame(ode(start, times, seirmod2,
          paras))
     ImatB[i,]=out$I
     start = c(S = out$S[12001], E = out$E[12001],
          I = out$I[12001], R = out$R[12001])
}
sel=seq(7001, 12000, by=120)
par(mfrow=c(1,1))
     plot(NA, xlim=range(mu),  ylim=range(ImatF[,sel]),
          log="y", xlab="mu", ylab="prevalence")
for(i in 1:101){
     points(rep(mu[i], dim(ImatF)[2]), ImatF[i, ],
          pch=20, cex=0.25)
     points(rep(mu[i], dim(ImatB)[2]), ImatB[i, ],
          pch=20, cex=0.25,col=2)
 }
```

In Fig. 5.6 the attractor from the "forward" analysis is shown in black and "backward" analysis in red. This color coding clearly reveals the coexisting attractors for a range of parameter values. The transition from annual to biennial epidemics predicted as μ varies between 15 per thousand per year and 25 per thousand per year is clearly seen following the baby boom post-World War II in the dynamics of measles in the UK (Sect. 6.5). The complex dynamics at lower susceptible recruitment rates, again, comes about because of dissonance between the external annual forcing and the internal periodic clock. With a *per capita* susceptible recruitment rate of 0.002/year which corresponds to 90% vaccination rate in our model, the dampening period is predicted to be 7.4 years. Earn et al. (2000b) predicted that vaccination may—depending on seasonality —lead to chaotic epidemics. A complication that makes this less likely in real populations is that the troughs following major epidemics are so deep that the chain of transmission will almost always break, leading to disease fade-out (Ferrari et al. 2008) (though see Sect. 10.2 for a counter example). In his mathematical study of rabies spread, Mollison (1991) dubbed this

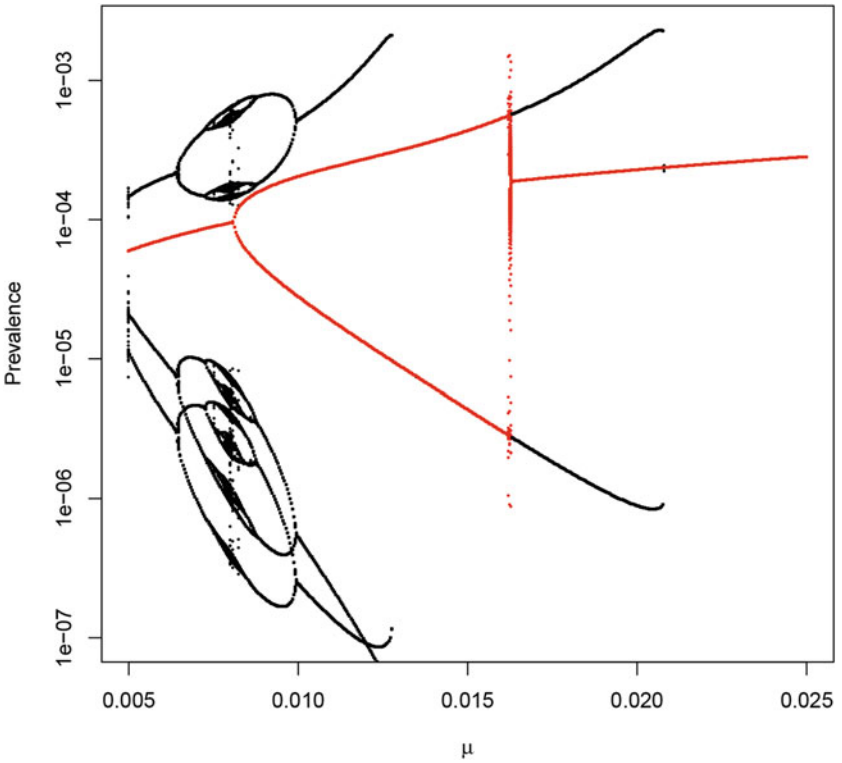

Fig. 5.6 The bifurcation plot of prevalence against birth rate μ for the forced SEIR model with intermediate seasonality. Black represents values from the "forward" analysis and red the "backward" analysis

the "atto-fox" of deterministic models; If the models predict that there is a 10^{-18}th of a rabid fox running around, deterministic predictions may not be very relevant to real-life epidemics.

5.7 ShinyApp

The seasonally forced SEIR model can be further studied using the `SEIR.app` in the `epimdr`-package. The app can be launched from R through:

```
require(shiny)
SEIR.app
```